SARS-CoV-2 spike-specific memory B cells express markers of durable immunity after non-severe COVID-19 but not after severe disease

Raphael A. Reyes[1], Kathleen Clarke[1], S. Jake Gonzales[1], Angelene M. Cantwell[1], Rolando Garza[1], Gabriel Catano[2], Robin E. Tragus[2], Thomas F. Patterson[2], Sebastiaan Bol[1], Evelien M. Bunnik[1]*

[1] Department of Microbiology, Immunology and Molecular Genetics, Long School of Medicine, The University of Texas Health Science Center at San Antonio, San Antonio, TX, USA

[2] Department of Medicine, Division of Infectious Diseases, The University of Texas Health Science Center at San Antonio, University Health System, San Antonio, TX, USA

[3] The South Texas Veterans Health Care System, San Antonio, TX, USA

***Correspondence**

Evelien M. Bunnik, Ph.D.

bunnik@uthscsa.edu

7703 Floyd Curl Drive

San Antonio, TX 78229

United States of America

+1 210-450-8146

Conflict of interest statement: The authors have declared that no conflict of interest exists.

Keywords: T-bet; FcRL5; adaptive immunity; humoral immune response; IgM; IgG

ABSTRACT

SARS-CoV-2 infection elicits a robust B cell response, resulting in the generation of long-lived plasma cells and memory B cells. Here, we aimed to determine the effect of COVID-19 severity on the memory B cell response and characterize changes in the memory B cell compartment between recovery and five months post-symptom onset. Using high-parameter spectral flow cytometry, we analyzed the phenotype of memory B cells with reactivity against the SARS-CoV-2 spike protein or the spike receptor binding domain (RBD) in recovered individuals who had been hospitalized with non-severe (n=8) or severe (n=5) COVID-19. One month after symptom onset, a substantial proportion of spike-specific IgG^+ B cells showed an activated phenotype. In individuals who experienced non-severe disease, spike-specific IgG^+ B cells showed increased expression of markers associated with durable B cell memory, including T-bet, FcRL5, and CD11c, which was not observed after severe disease. Five months post-symptom onset, the majority of spike-specific memory B cells had a resting phenotype and the percentage of spike-specific $T\text{-}bet^+$ IgG^+ memory B cells decreased to baseline levels. Collectively, our results suggest that the memory B cell response elicited during non-severe COVID-19 may be of higher quality than the response after severe disease.

INTRODUCTION

Severe acute respiratory syndrome coronavirus 2 (SARS-CoV-2) is responsible for the global coronavirus disease 2019 (COVID-19) pandemic resulting in more than 4 million deaths reported worldwide as of September 2021 (1). Highly efficacious vaccines have limited SARS-CoV-2 transmission and significantly reduced morbidity and mortality in regions of the world with access to these vaccines. However, the majority of the world's population lives in areas with low vaccination rates and remain at higher risk of SARS-CoV-2 infection and COVID-19. Both vaccination and natural infection elicit immunological protection against SARS-CoV-2 (re-)infection. Although mRNA vaccination elicits higher antibody titers and more diverse antibody responses against the SARS-CoV-2 spike protein than natural infection (2, 3), results from the first longitudinal studies in unvaccinated individuals with prior COVID-19 suggest that naturally acquired immune responses are maintained for at least a year after infection and that these responses protect from subsequent re-infection (4-11). Because many people remain unvaccinated, it will be important to understand the immune response elicited by natural infection and whether the durability of naturally acquired immunity is influenced by the severity of disease.

Although SARS-CoV-2 infection elicits robust responses in both the T cell and B cell arms of the adaptive immune system (12, 13), the majority of research efforts have focused on B cell and antibody responses, which are thought to be critical for the control of infection and protection against re-infection. Humoral immune responses against pathogens consist of multiple components. The early B cell response is dominated by short-lived antibody-secreting cells, called plasmablasts. Simultaneously, other B cell populations undergo selection for high affinity antigen-binding in germinal centers of the secondary lymphoid organs, and can differentiate into long-lived, antibody-secreting plasma cells that migrate to the bone marrow or into memory B cells that remain in the circulation (reviewed in (14)). COVID-19 patients rapidly generate potent

neutralizing IgG antibodies against the spike protein (15, 16). Anti-spike antibody titers peak within the first two months post-infection, decline in the subsequent 3 – 4 months, and then plateau at titers higher than those detected in pre-pandemic samples, but are lower than anti-spike antibody titers elicited by vaccination (3, 5, 7, 17). These phases of the anti-spike IgG profile in the circulation are the result of early short-lived plasmablast responses, followed by the secretion of antibodies by longer-lived bone marrow plasma cells (5). In addition, spike-specific IgG^+ memory B cells are maintained or even increase in numbers for at least six months to one year following SARS-CoV-2 infection (6-8, 18). Analysis of monoclonal antibodies obtained from these memory B cells revealed continued evolution of the B cell response over time, as evidenced by higher levels of somatic hypermutation, resulting in increased binding affinity and neutralizing capacity (7, 19, 20).

In recent years, novel subsets of activated B cells and memory B cells have been identified. These novel B cell subsets have mainly been defined by their phenotype, that is, the collection of markers expressed on their cell surface or intracellularly, and are thought to possess either protective or pathogenic functions in the immune response. For example, several subsets of double negative (DN; $CD27^-$ IgD^-) B cells have been defined in recent years (21, 22). Type 1 double negative cells (DN1 cells), defined as DN cells that express CXCR5 or CD21 and lack CD11c and FcRL5, are transcriptionally similar to class-switched memory B cells and seem to be part of a functional B cell response (21, 23). On the other hand, type 2 DN cells (DN2 cells), defined as $CD11c^+$/$FcRL5^+$ and $CXCR5^-$/$CD21^-$ DN cells, are thought to arise from the activation of naïve B cells outside of the B cell follicle in the lymph node. Type 3 DN cells (DN3 cells), defined as $CD11c^-$/$FcRL5^-$ and $CXCR5^-$/$CD21^-$ DN cells, have also been associated with this extrafollicular response and may be DN2 cell precursors (22, 23). DN2 cells are more abundant in patients with autoimmune disorders, such as systemic lupus erythematosus, and are thought to differentiate into auto-antibody-secreting cells. DN2 cells are also observed in the circulation

of patients with severe COVID-19 (22), an observation that has been linked to lack of germinal center formation, presumably leading to an impaired B cell response (24).

Interestingly, memory B cells ($CD27^+$ IgD^-) expressing some of the same markers as DN2 cells, including CD11c and FcRL5, as well as the transcription factor T-bet, have been described as part of normal, functional immune responses (25, 26). Specifically, these cells have been implicated in long-lived B cell memory after tetanus toxoid and influenza virus vaccination (27, 28). In recovered COVID-19 patients, memory B cells present 1 – 3 months after symptom onset are also found to express FcRL5 and T-bet, suggesting that these markers may delineate a subset of long-lived memory B cells against SARS-CoV-2 (13, 29). However, it is unclear whether disease severity influences the development of memory B cells that express T-bet or FcRL5, and whether the phenotype of memory B cells changes with the continued evolution of this B cell compartment in the months following SARS-CoV-2 infection. A more detailed analysis of B cell subsets in recovered COVID-19 patients will therefore be needed to acquire insight into the early B cell response and the evolution of memory B cells over time.

Here, we performed spectral flow cytometry to characterize the phenotype of SARS-CoV-2-specific B cells in unvaccinated patients who recovered from non-severe or severe COVID-19. We focused on two comparative analyses. First, we compared the phenotype of spike-specific B cells between convalescent patients who were hospitalized with non-severe and severe disease to determine whether the B cell response developed differently in these two groups. Second, we compared the phenotype of memory B cells shortly after recovery to that at five months post-symptom onset to analyze the ongoing evolution of the B cell response. The results from this study provide insight into naturally acquired B cell memory against SARS-CoV-2 and a better understanding of the characteristics of durable B cell immunity.

RESULTS

Study criteria

Study participants (n=16) were enrolled in the Adaptive COVID-19 Treatment Trial (ACTT)-1 or ACTT-2 clinical trials which were designed to evaluate the effect of remdesivir or baricitinib plus remdesivir for the treatment of COVID-19 in hospitalized patients (30, 31). Participants identified predominantly as white (94%) and Hispanic (75%), and all except one individual had one or more comorbidities (**Table S1**). Participants were classified as non-severe (n = 11) or severe (n = 5) COVID-19 cases based on their worst ordinal score for disease severity during hospital stay. In summary, non-severe cases did not require supplemental oxygen (score = 4) or required supplemental oxygen or non-invasive ventilation (score = 5 or 6), while severe cases needed invasive mechanical ventilation (MV) or extracorporeal membrane oxygenation (ECMO) (score = 7). The definition of severe disease was made based on the need for MV or ECMO, because this distinguishes the most critical patients, who are the most likely to develop impaired immune responses (24, 32). Blood was collected after discharge from the hospital (a median of 30 days after symptom onset for non-severe cases (n = 8) and 32 days after symptom onset for severe cases (n = 5)) (**Figure 1**). For participants with non-severe disease, additional samples were collected at an earlier time point (a median of 18 days post-symptom onset; n = 9) and at a follow-up visit approximately 5 months post-symptom onset (median, 147 days; n = 7) based on availability and consent. Peripheral blood mononuclear cells (PBMCs) from healthy donors (n = 3) collected before the start of the pandemic (2018 or early 2019) were used as negative controls.

The proportions of B cell subsets in convalescent patients are similar between non-severe and severe COVID-19 cases

Severe COVID-19 is associated with an extrafollicular B cell response characterized by a high percentage of DN2 B cells in the circulation, similar to what is observed in patients with

autoimmune disorders (21, 22). Previous data suggest that the percentage of DN2 B cells in patients with severe COVID-19 had returned to normal levels approximately 1.5 months after hospital discharge (33). To determine whether COVID-19 severity affects the distribution of B cell subsets shortly after recovery (four to five weeks after symptom onset), we analyzed the relative proportions of B cell subsets individuals who recovered from non-severe (n = 8) or severe (n = 5) disease by spectral flow cytometry using an antibody panel against 19 cell surface and intracellular markers (**Table S2**). B cells were first gated on live, $CD19^+$ $CD20^+$ $CD38^{-/lo}$ cells to exclude transitional B cells and antibody-secreting cells, and were subsequently divided into naïve ($CD27^-$ IgD^+), unswitched memory ($CD27^+$ IgD^+), resting switched memory ($CD27^+$ IgD^- $CD21^+$), activated switched memory ($CD27^+$ IgD^- $CD21^-$) and double negative (DN; $CD27^-$ IgD^-) B cells (**Figure 2A**). Apart from a significant increase in the percentage of unswitched memory B cells in individuals who had experienced severe disease compared to those with non-severe COVID-19, no differences in the distribution of these B cell subsets were observed between the two groups of recovered COVID-19 patients (**Figure 2B-C, Figure S1A**). Among DN cells, DN1 ($FcRL5^-$ $CXCR5^+$) B cells were the dominant subset in both groups of recovered COVID-19 patients, and we did not detect significant differences in the frequencies of DN1, DN2 ($FcRL5^+$ $CXCR5^-$), and DN3 ($FcRL5^-$ $CXCR5^-$) B cells between the two groups (**Figure 2D, Figure S1B**). In combination with previous reports (22, 33), these results suggest that expansion of the DN2 B cell population during severe COVID-19 might be transient and that these cells disappear soon after recovery.

The percentage of spike-specific and RBD-specific B cells and their isotype distributions are similar between non-severe and severe cases

Our flow cytometry panel also included antigen probes to detect B cells reactive with the SARS-CoV-2 spike protein and the spike receptor binding domain (RBD). RBD is the part of the spike protein that interacts with angiotensin-converting enzyme 2, the viral receptor on host cells, and

is the dominant target of neutralizing antibodies (34). However, the majority of antibodies generated against the spike protein bind to epitopes outside RBD (35). Whereas the RBD sequence is highly specific for SARS-CoV-2 (36), the non-RBD parts of spike, in particular the S2 subunit, share epitopes with other coronaviruses that circulate in the human population (37-39). Evidence for pre-existing memory B cells that are cross-reactive with other coronaviruses has been reported (40). Because pre-existing immunity could affect the development of the immune responses against these two parts of the spike protein, we analyzed B cell responses against RBD and non-RBD spike epitopes separately.

We constructed spike tetramers in two fluorochrome formats and defined the population of cells staining positive for both tetramers as spike-specific (**Figure 3A**). The spike-specific B cells were then divided into non-RBD-specific and RBD-specific B cells based on reactivity with the RBD tetramer (**Figure 3A**). Non-RBD-specific and RBD-specific B cells were strongly enriched for antigen-experienced B cells (**Figure 3B,** compare to **Figure 2B**), with no statistically significant differences in the proportions of various B cell populations between individuals who recovered from non-severe or severe disease (**Figure 3B, Figure S2**). In addition, reactivity against spike and RBD tetramers among control donor B cells was minimal (**Figure 3A,C**), suggesting that these probes selectively bind to antigen-specific B cells.

The percentage of spike-specific B cells among antigen-experienced B cell populations (unswitched memory, switched memory, and DN B cells) among all patients ranged from 0.1% to 1.8% (median, 0.6%) (**Figure 3C**). One donor (marked with # in Figure 3C) had only six spike-specific B cells and was therefore not included in subsequent analyses that required further subsetting of these cells. All other donors had between 42 and 450 spike-specific B cells. In line with a previous study (4), a median of 22% of spike-specific B cells were reactive against RBD (**Figure 3D**). Ogega *et al*. recently reported that patients who recovered from severe

COVID-19 harbored more RBD-specific B cells than COVID-19 patients who never required hospitalization (29). We did not observe a difference in the percentage of RBD-specific cells between individuals who recovered from non-severe and severe disease, potentially because our non-severe group had been hospitalized and suffered from more severe disease than the group with non-severe disease in the Ogega *et al.* study.

Next, we compared the isotype of class-switched spike-specific B cells between patients who recovered from non-severe and severe COVID-19 by categorizing spike-specific antigen-experienced B cells based on IgM, IgG, or IgA expression. The percentage of IgM^+, IgG^+, and IgA^+ class-switched B cells among spike-specific B cells did not differ significantly between the two patient groups and in both groups, the majority of class-switched spike-specific B cells were IgG^+ (**Figure 3E**). We also determined plasma IgM and IgG reactivity to the spike protein and RBD and observed no significant differences in IgM or IgG titers to the spike protein or RBD between convalescent patients who recovered from non-severe or severe disease (**Figure 3F**). Collectively, these results suggest that individuals who recovered from either non-severe or severe COVID-19 have similar immune responses to the SARS-CoV-2 spike protein, in terms of the prevalence of spike-specific B cells and their major phenotype.

Non-severe COVID-19 is associated with an increased population of T-bet$^+$ spike-specific IgG$^+$ B cells

To gain deeper understanding of the differences in memory B cell responses between individuals who had either non-severe or severe COVID-19, we combined the acquired flow cytometry data for all 19 markers (**Table S2**) of all individuals and plotted a composite image using Uniform Manifold Approximation Projection (UMAP). UMAP clusters cells in a 2D plot based on similarity in phenotype and therefore provides meaningful organization of cell subsets. For each recovered COVID-19 patient, we took a random sample of cells (n = 10,000) and

projected the spike-specific antigen-experienced B cells onto the composite UMAP (**Figure 4A**). We also plotted contours for various B cell subsets to visualize their location within the UMAP (**Figure 4B,** see **Figure S3** for heatmaps of all individual markers overlaid on the composite UMAP). The composite image shows differences in the location of spike-specific B cells, predominantly among IgG^+ B cells (**Figure 4A, B**). The large majority of IgG^+ B cells are memory B cells, but a small fraction of these cells are DN1 B cells that are thought to contribute to a functional immune response and were therefore included in a phenotypic analysis of spike-specific IgG^+ B cells.

Irrespective of disease severity, spike-specific IgG^+ B cells expressed increased levels of activation markers CD80, Ki-67, and CD95 (**Figure 4C**) compared to all IgG^+ B cells, with no differences between the two groups. In contrast, spike-specific IgG^+ B cells after non-severe disease showed an increase in the expression of the transcription factor T-bet that was not seen after severe disease (**Figure 4D**). A median of 28% of spike-specific IgG^+ B cells in individuals who experienced non-severe disease expressed T-bet, which has been associated with strong anti-viral immunity (41). Conversely, T-bet was expressed in only about 10% of spike-specific IgG^+ memory B cells in individuals who recovered from severe disease (**Figure 4D**). $T\text{-}bet^+$ cells often have a distinct cell surface marker profile, including expression of CD11c and FcRL5 and the absence of CD21 (25, 26, 28) . Indeed, in addition to T-bet, the percentage of both $FcRL5^+$ and $CD11c^+$ spike-specific IgG^+ memory B cells was increased among spike-specific IgG^+ B cells in patients who recovered from non-severe COVID-19 as compared to all IgG^+ B cells in these patients (**Figure 4D**), while these differences were not seen in individuals who recovered from severe COVID-19. Conversely, a lower percentage of $CD21^+$ spike-specific IgG^+ B cells was observed after non-severe disease but not after severe disease (**Figure 4D**). To confirm that the measurement of T-bet, FcRL5, CD11c, and CD21 expression was robust between experiments, we processed and analyzed technical replicates for samples from one non-severe

and one severe case on different days, and observed almost perfect correlation between the replicates (Spearman r = 0.99, P = 0.0002, **Figure S4**). We then analyzed the combinatorial expression of these markers by combining spike-specific IgG$^+$ T-bet$^+$ B cells from all donors and plotting contour plots depicting the expression of FcRL5, CD11c, CD21, CD27, CXCR3, and CXCR5 (**Figure 5**). This revealed four subpopulations of T-bet$^+$ IgG$^+$ B cells, of which cells expressing FcRL5, CD11c, CD27 and CXCR3, and lacking CD21 and CXCR5 (type I; activated switched memory B cells) were most abundant in both non-severe and severe cases (**Figure 5**). This phenotype has previously been observed in activated B cells after influenza virus vaccination and is thought to delineate a B cell subset associated with long-lived humoral immunity (26, 28, 41). Collectively, the higher prevalence of spike-specific B cells that express markers associated with durable immunity in individuals who recovered from non-severe COVID-19 than in those who experienced severe disease suggests that disease severity influences the quality of the B cell response.

SARS-CoV-2 spike-specific memory B cells return to a resting phenotype with baseline levels of T-bet expression five months post-symptom onset

Activated T-bet$^+$ B cell subsets have been shown to expand and contract rapidly following influenza virus vaccination, peaking between 14 and 28 days post-vaccination and returning to baseline levels after three months (25). In addition, it has been shown that the memory B cell response continues to mature up to one year following SARS-CoV-2 infection, giving rise to B cell clones with higher levels of somatic hypermutation and resulting in increases in antigen-binding affinity and ability to neutralize the virus (7, 19, 20). To evaluate the early dynamics of T-bet$^+$ spike-specific B cells and continued development of the phenotype of memory B cells in parallel with ongoing selection and maturation, we analyzed additional blood samples from recovered COVID-19 patients with non-severe disease collected at an earlier time point (median, 19 days post-symptom onset) (T1, **Figure 1**) and at a follow-up visit five months post-

symptom onset (T3, **Figure 1**). Unfortunately, we were unable to recruit any individuals who had experienced severe disease for a follow-up visit at five months post-symptom onset. In addition, at the earlier time point, most individuals with severe disease were still hospitalized (**Figure 1**). We therefore limited this analysis to individuals who recovered from non-severe COVID-19.

The percentages of total naïve, unswitched memory, resting switched memory, activated switched memory, and double negative B cell subsets among total B cells did not differ between the two time points (**Figure S5**). However, the phenotype of spike-specific B cells changed considerably between the two early time points and five months post-symptom onset (**Figure 6A, Figure S6**), as described in further detail below. Similar to what has been reported by Dan *et al.* and Sokal *et al.* (4, 8), the percentage of spike-specific B cells among antigen-experienced B cells remained relatively stable at five months post-symptom onset (**Figure 6B**). In addition, the reactivity against RBD among these spike-specific B cells increased between 2 – 3 weeks and 4 – 5 weeks post-symptom onset, but did not change at the 5-month time point (**Figure 6C**). The larger proportion of non-RBD-specific B cells early in infection may be the result of recall responses of pre-existing memory B cells that are cross-reactive with other coronaviruses.

The percentage of antigen-experienced spike-specific B cells with an unswitched memory B cell phenotype was reduced at the 5-month time point (**Figure 6D**). The percentage of spike-specific activated switched memory B cells drastically decreased over time, accompanied by an increase in resting memory B cells (**Figure 6E**). Among switched memory B cells, the percentage of IgM^+ and IgA^+ memory B cells declined and the proportion of IgG^+ memory B cells increased at five months post-symptom onset (**Figure 6F**). In line with the decrease of IgM^+ memory B cells, the anti-spike and anti-RBD plasma IgM responses were lost almost completely at five months post-symptom onset. Plasma IgG titers against the spike protein remained stable, whereas plasma IgG titers against RBD showed a modest decrease (**Figure 6G**). These results

299 indicate that both the unswitched plasma cell and memory B cell response against the spike
300 protein are short-lived, while the class-switched IgG$^+$ response is more durable, as has been
301 reported by others (4, 8).
302
303 Both the decrease of unswitched memory B cells and the change from an activated to a resting
304 switched memory B cell phenotype can be seen in composite UMAPs of the three time points
305 (**Figure 7A-B**). In line with the return to a resting memory B cell phenotype, expression of
306 CD80, Ki-67, and CD95 was decreased at 20 – 23 weeks post-symptom onset as compared the
307 two earlier time points (**Figure 7C**). The percentage of CD80$^+$ spike-specific IgG$^+$ B cells at 20 –
308 23 weeks post-symptom onset still showed an increase over baseline levels (P = 0.016,
309 Wilcoxon signed rank test), while expression of Ki-67 and CD95 had returned to levels seen in
310 non-spike-specific IgG$^+$ B cells (**Figure 7C, Figure S7**). The expression of T-bet was higher at 2
311 – 3 weeks post-symptom onset than at 4 – 5 weeks post-symptom onset (median, 58% and
312 28%, respectively), although this difference was not statistically significant, and decreased
313 further to baseline levels (~ 10%) at 20 – 23 weeks post-symptom onset (**Figure 7D,E**). Similar
314 dynamics were observed for FcRL5 and CD11c, while CD21 expression increased significantly
315 over time (**Figure 7E**). The percentage of type I T-bet$^+$ spike-specific IgG$^+$ B cells (activated
316 switched memory B cells) that dominated the early response decreased dramatically over time
317 (**Figure 7D**). Instead, the T-bet$^+$ spike-specific IgG$^+$ B cells present at five months post-symptom
318 onset were mainly type II (FcRL5$^+$ CD11c$^+$ CD21$^-$ CD27$^-$, DN2 B cells) and type IV (FcRL5$^-$
319 CD11c$^-$ CD21$^+$ CD27$^+$, resting switched memory B cells) subsets, making up ~35% and ~40% of
320 T-bet$^+$ spike-specific IgG$^+$ B cells, respectively. These results suggest that the memory B cell
321 response continues to evolve until at least five months after infection. In addition, the decrease
322 of T-bet$^+$ spike-specific B cells in the circulation over the course of five months post-symptom
323 onset suggests that their abundant presence in the blood may signify recent exposure.
324

DISCUSSION

In the current COVID-19 pandemic, an important question that has only partially been answered is whether SARS-CoV-2 infection elicits durable immunity. Assessments of B cell responses up to one year post-infection suggest that both neutralizing antibodies and memory B cells against the SARS-CoV-2 spike protein remain detectable in the circulation of most recovered COVID-19 patients and are stable or decay slowly at this time point. In this study, we aimed to better understand the memory B cell response and to determine whether the severity of COVID-19 disease course influences the development of B cell responses. Using high-parameter spectral flow cytometry, we analyzed the phenotype of B cells reactive with both non-RBD and RBD epitopes on the spike protein shortly after recovery and approximately five months post-symptom onset.

Our study consisted of a relatively small number of individuals but recapitulated many of the observations reported from much larger cohorts, including the frequency of spike-specific memory B cells after infection and the fraction of spike-specific B cells that recognizes RBD epitopes. We also confirmed the loss of IgM^+ and IgA^+ spike-specific memory B cells and anti-spike and anti-RBD plasma IgM, as well as maintenance of IgG^+ spike-specific memory B cells and anti-spike plasma IgG five months post-symptom onset (4, 17). This gives us confidence in the validity of several new observations that we discuss in more detail below.

The most striking result from this study is the higher percentage of spike-specific IgG^+ B cells that express the transcription factor T-bet in individuals who recovered from non-severe disease as compared to those who recovered from severe disease. Previously, it was observed that a higher percentage of total $CD19^+$ $T\text{-}bet^+$ $IgG_1{}^+$ B cells was associated with shorter symptom duration (42). Here, we determined that this association predominantly involves SARS-CoV-2 antigen-specific B cells, suggesting implications for the development of B cell memory. The

351 expression of T-bet, in parallel with a surface marker profile that includes the presence of FcRL5
352 and CD11c and the absence of CD21, has previously been reported on activated B cells shortly
353 after vaccination and infection, and is associated with long-lived humoral immunity (26, 28, 41).
354 Here, we observed that an increased percentage of spike-specific B cells showed this activated
355 phenotype shortly after recovery from non-severe COVID-19, but not after severe COVID-19.
356 Ogega *et al*. reported higher FcRL5 expression on RBD-specific class-switched memory B cells
357 after non-severe COVID-19 (non-hospitalized patients) than after severe disease (hospitalized
358 patients) (29), findings that are in agreement with our results. In addition, higher levels of
359 somatic hypermutation were observed in IgG^+ memory B cells following non-severe COVID-19
360 than severe disease (43), while patients who died from COVID-19 showed an absence of
361 germinal centers and a delay in the development of neutralizing antibodies (24, 44). Collectively,
362 these data are indicative of functional development of B cell immunity with germinal center
363 responses in patients with non-severe disease, as compared to a more dysfunctional B cell
364 response in severe disease cases.
365
366 T-bet expression in B cells can be induced by interferon gamma (IFNγ) signaling through the
367 IFNγ receptor (45, 46). IFNγ plays an important role in the immune response against viral
368 infections. Although many contradictory findings have been reported about the role of INFγ in
369 SARS-CoV-2 infection, the induction of INFγ early in infection seems important in the control of
370 viral replication [summarized in (47)]. Indeed, low IFNγ and low induction of interferon-
371 stimulated genes contribute to the development of COVID-19 (48). Failure to control viral load
372 leads to the induction of a hyper-inflammatory response later in disease, in parallel with
373 persistent high levels of IFNγ. However, these conditions may not promote the development of
374 T-bet^+ memory B cells. Instead, patients with severe disease show a strong extrafollicular B cell
375 response, resulting in an accumulation of DN2 B cells [(22)]. In our study, no difference was
376 observed in the percentage of DN2 B cells shortly after recovery between patients with either

non-severe or severe disease, suggesting that these DN2 B cells may be relatively short-lived. Of note, DN2 cells typically also express T-bet (21), highlighting that the expression of this transcription factor alone is not the determining factor in the development of either a functional or pathogenic B cell response. The difference that we observed in the percentage of T-bet$^+$ spike-specific IgG$^+$ B cells between patients recovered from non-severe or severe COVID-19 could reflect these two developmental pathways of anti-viral immune responses.

In individuals who experienced non-severe COVID-19, T-bet$^+$ spike-specific IgG$^+$ B cells almost disappeared from the circulation five months post-symptom onset. This is in line with the transient peak of activated memory B cells observed after influenza vaccination (25, 26). The cell surface marker expression profile and dynamics of the T-bet$^+$ B cells detected in this study matches best with the AM2 subset of activated memory B cells defined by Andrews *et al*., which peaked 14 days after influenza vaccination and had almost disappeared 90 days post-vaccination (25). However, this does not necessarily mean that these cells are short-lived. It was recently shown that the spleen harbors a population of resident T-bet^{hi} memory B cells with specificity to viral antigens (49). In addition, it has been reported that T-bet^{hi} memory B cells elicited in response to influenza virus vaccination rapidly differentiated into antibody-secreting cells upon reactivation one year later (28). T-bet$^+$ memory B cells thus seem to contribute to effective recall responses upon re-exposure, but may only be detectable in the circulation shortly after infection. In this regard, it is important to point out that the timing of sampling can strongly affect the frequency of transient B cell populations, and samples selected for comparative analyses need to be carefully matched to account for rapid changes in the abundance of activated B cell populations over time. For example, this may explain the discrepancy between this study and the observation by Sokal *et al*. that T-bet expression in spike-specific B cells was higher in individuals with severe COVID-19 than individual with non-severe COVID-19 (8). In the Sokal *et al.* study, samples from severe cases were collected at an

403 earlier time point than those from non-severe cases (median, 18.8 days versus 35.5 days post-
404 symptom onset), which could have influenced these results (8).
405
406 Thus far, no differences have been observed in serum anti-spike antibody titers, *in vitro* serum
407 neutralizing activity, or percentages of spike-specific memory B cells between non-severe and
408 severe COVID-19 patients in the months after infection (18). It remains to be determined
409 whether the durability of B cell memory differs between individuals who experienced non-severe
410 or severe disease. We speculate that individuals who recovered from non-severe disease
411 develop a higher quality memory B cell response that may be longer-lived or may give rise to a
412 larger population of antibody-secreting cells upon re-exposure. An alternative interpretation of
413 the paucity of T-bet$^+$ spike-specific memory B cells in patients with severe disease could be that
414 a robust T-bet$^+$ B cell response protects against severe COVID-19. Although patients who died
415 from COVID-19 show defects in the development of B cell responses (24, 44), it is likely that the
416 expansion of a population of T-bet$^+$ spike-specific memory B cells is a consequence of the
417 immune environment during disease, not a factor contributing to survival. We believe these cells
418 are a sign of a balanced immune response that contributes to viral clearance through the
419 production of neutralizing antibodies and leads to the development of durable B cell memory,
420 but that T-bet$^+$ memory B cells do not play a direct role in protection against severe disease.
421
422 In conclusion, we have shown that the memory B cell response against SARS-CoV-2 spike
423 protein develops differently in patients with non-severe disease compared those with severe
424 disease, with more spike-specific B cells that express a B-cell marker profile associated with
425 durable immunity, characterized by expression of T-bet, FcRL5, and CD11c, and low expression
426 of CD21 in individuals who recovered from non-severe COVID-19. Although antibody titers or
427 percentage of spike-specific memory B cells up to one year are similar or higher in individuals
428 who recovered from severe disease as compared to non-severe cases (8, 18), the increased

429 percentage of B cells associated with long-lived immunity in non-severe COVID-19 patients may
430 have consequences for long-term immunity against SARS-CoV-2 re-infection or severity of the
431 resulting disease. T-bet$^+$ spike-specific B cells nearly disappeared from the circulation five
432 months post-symptom onset, consistent with loss of these cells from the periphery or migration
433 into tissues. These data aid in the understanding of naturally acquired B cell responses against
434 SARS-CoV-2 and help characterize the B cell populations that may be responsible for durable,
435 long-lived immunity.
436

METHODS

Isolation of plasma and peripheral blood mononuclear cells

Blood from recovered COVID-19 patients was processed within four hours of blood draw. Plasma was separated from cells by centrifugation at 250 × g for 5 min at room temperature (RT). Plasma was depleted of platelets by centrifugation at 2,000 × g for 15 min at 4°C and was stored at -20°C. Peripheral blood mononuclear cells (PBMCs) were isolated from the cellular fraction as described below. PBMCs used as negative controls were collected in 2018 and early 2019 by isolation from buffy coats (Interstate Blood Bank, Memphis, TN) obtained the day following blood draw. Buffy coats were stored and shipped at room temperature (RT) and processed immediately upon arrival. Cells were diluted approximately 4 × in PBS with 2 mM EDTA. PBMCs were layered on Ficoll-Paque (GE Healthcare, cat. no. 17144002) and spun at 760 × g for 20 min at RT to pellet erythrocytes and separate leukocytes. The leukocytes were then washed in PBS with 2 mM EDTA, centrifuged at 425 × g for 15 min at RT, followed by centrifugation at 250 × g for 10 min at RT for all subsequent wash steps necessary to remove all platelets, determined by cloudiness of the supernatant. Next, PBMCs were resuspended in cold IMDM/GlutaMAX (Gibco, cat. no. 31980030) supplemented with 10% heat-inactivated, USA-sourced, fetal bovine serum (FBS) and 5% cell culture grade DMSO, counted, and cryopreserved in the liquid nitrogen vapor phase.

Spike and RBD protein production and tetramer synthesis

Recombinant SARS-CoV-2 HexaPro spike and RBD were produced from Addgene plasmid #154754 (50) and BEI plasmid NR-52309, respectively, for use in ELISA experiments. DNA plasmids were purified from DH5alpha Competent Cell (Zymo, cat. no. T3007) cultures using a ZymoPURE II Plasmid Maxiprep (Zymo, cat. no. D4203). 25 µg plasmid was used to transfect 25 ml Expi293F (Thermo, cat. no. A14635) culture per manufacturer's instructions. Culture supernatants were collected 5 days post-transfection. His-tagged S and RBD were purified

using HiTrap chelating high performance columns (Cytiva, cat. no. 17-0408-01) charged with Ni^{2+}, washed with PBS (pH 7.2), and eluted with 0.3 M imidazole in PBS (pH 7.2). The imidazole was removed from the eluted protein buffer using a HiPrep desalting column (Cytiva, cat. no. 17-5087-01). The protein was concentrated using a 30 kDa MWCO Amicon ultra-15 centrifugal filter (Sigma, cat. no. UFC903024), and stored at -70°C. For the production of biotinylated S and RBD protein used for the synthesis of antigen tetramers, Addgene plasmid #154754 and BEI plasmid NR-52309 were altered to include a biotinylation site. The modified plasmids have been deposited to Addgene: #166856 and #166857 for spike and RBD, respectively. Cells were co-transfected with either plasmid #166856 or #166857 and a plasmid encoding BirA ligase (Addgene #32408) at a 4:1 ratio (m/m). 100 mM D-biotin (Sigma, cat. no. B4639) was added immediately post-transfection to a final concentration of 10 mM. Spike and RBD tetramers were synthesized by incubating biotinylated protein with fluorophore-conjugated streptavidin overnight at 4°C (streptavidin-PE, Tonbo, cat. no. 50-4317-U100, streptavidin-APC, Tonbo, cat. no. 20-4317-U100, streptavidin-BV421, BioLegend, cat. no. 405226) at a molar ratio of 5:1, respectively, to generate three individual tetramers: spike-PE, spike-APC, and RBD-BV421.

Protein gels

As a quality control step, purified spike and RBD proteins were visualized on a polyacrylamide gel (**Figure S8**). 800 ng of protein was loaded on a 4 – 12% Bis-Tris gel (Thermo, cat. no. NP0321BOX) after it was mixed with 2× Laemmli loading buffer and incubated at 85°C for 5 min. The gel was run with MOPS running buffer (Thermo, cat. no. NP0001) at 200 V for 50 min after which the proteins were stained using Imperial Protein Stain (Thermo, cat. no. PI24615) per manufacturer's instructions.

B cell isolation and staining

Cryopreserved PBMCs were thawed in a water bath set at 37°C and immediately mixed with pre-warmed thawing medium (IMDM/GlutaMAX supplemented with 10% heat inactivated FBS and 0.01% Universal Nuclease (Thermo, cat. no. 88700). After brief centrifugation (250 × g, 5 min) at RT, the cell pellet was resuspended in warm thawing medium and viable cells were counted using trypan blue on a Cellometer Mini (Nexcelom) automated cell counter. Next, the PBMCs were pelleted (250 × g, 5 min, RT), resuspended in isolation buffer (PBS supplemented with 2% heat inactivated FBS and 1 mM EDTA) at 50 million live cells/ml, and filtered through a 35 µm sterile filter cap (Corning, cat. no. 352235) to break apart any aggregated cells. B cells were isolated using the EasySep Human B Cell Isolation Kit (StemCell, cat. no. 17954) according to manufacturer's instructions. After washing with cold PBS (250 × g, 5 min, RT), the isolated B cells were incubated with 1 µl Zombie UV Fixable Viability kit (Biolegend, cat. no. 423107) per 1 ml cell suspension for 30 min on ice. Cells were subsequently washed with cold PBS with 1% bovine serum albumin (BSA), followed by an incubation at 4°C for 30 min with an antigen tetramer cocktail (**Table S2**). Next, the cells were washed again with cold PBS with 1% BSA and incubated at 4°C for 30 min with a B cell surface marker antibody cocktail (**Table S2**), after which the cells were washed again with cold PBS with 1% BSA and resuspended in 1 ml Transcription Factor Fix/Perm Concentrate (Tonbo, part of cat. no. TNB-0607-KIT) diluted with 3 parts Transcription Factor Fix/Perm Diluent (Tonbo) and incubated at 4°C for 1 hour. After the incubation, the cells were washed twice with 3 ml of 1× Flow Cytometry Perm Buffer (Tonbo) and resuspended in intracellular marker antibody cocktail (**Table S2**) diluted in 1× Flow Cytometry Perm Buffer. After an incubation at 4°C for 30 min., the cells were washed twice with 3 ml 1× Flow Cytometry Perm Buffer and once with 3 ml cold PBS + 1% BSA. The cells were then fixed by adding 4% formaldehyde at a 1:1 ratio to sample (v/v), washed with 3 ml cold PBS + 1% BSA, and resuspended to 20 – 30 million cells/ml in PBS with 1% BSA, and filtered into a FACS tube through a 35 µm sterile filter cap. Cells were analyzed by flow cytometry immediately following fixation.

515

516 **Flow cytometry analysis**

517 B cells were analyzed on a Cytek Aurora spectral flow cytometer equipped with five lasers.
518 SpectroFlo QC Beads (Cytek, cat. no. SKU N7-97355) were run prior to each experiment for
519 performance tracking. Quality control and LJ tracking reports were used to ensure machine
520 performance and settings between different runs were comparable. B cells isolated from control
521 PBMCs collected pre-pandemic were used for the compensation of the live/dead stain and for
522 the unstained control. UltraComp eBeads (Thermo, cat. no. 01-2222-41) were used for
523 compensation of all other single stain fluorophores. FlowJo was used for gating and quantifying
524 cell frequencies. The cytometry analysis software OMIQ was used for the integration and
525 dimension reduction analysis. In short, Uniform Manifold Approximation and Projection (UMAPs)
526 where created by first pre-gating single/live/CD19^{+}/CD20^{+}/CD38^{lo} cells. Features used for
527 UMAP projection included mean fluorescence intensity of staining markers, excluding live/dead,
528 RBD, spike1, and spike2 with default parameters (neighbors = 15, metric = Euclidean, random
529 seed = 9889) and included all COVID-19 samples used in this study for initial projection.
530 Subsequently, files were subsampled to include an equal representation of cells from each
531 donor and concatenated within each group. For the projection of B cell subsets, Ig isotypes, and
532 antigen-specific B cells onto the UMAP, gates were manually set to identify populations of
533 interest using two-dimensional displays, which were then overlaid onto the UMAP projection.

534

535 **Detection of spike protein and receptor binding domain using an enzyme-linked**
536 **immunosorbent assay**

537 96-well plates (Corning, cat. no. 07-200-721) were coated with 50 µl of SARS-CoV-2 spike or
538 RBD at a concentration of 2 µg per ml in PBS and incubated overnight at 4ºC. An additional
539 plate was coated with goat anti-human IgG (Sigma, cat. no. I2136-1ML) at 4 µg/ml and IgM
540 (Sigma, cat. no. I1636-2ML) at 8 µg/ml, and served as a positive control. Plates were washed

twice using a gentle stream of deionized water from a faucet and subsequently incubated with 200 µl blocking buffer (PBS with 0.01% Tween-20 (Fisher, cat. no. BP337-100) and 3% non-fat dry milk (SACO)) for 1 hour at RT. Three-fold serial dilutions of 20 µg/ml human IgG or IgM were prepared in dilution buffer (PBS with 0.01% Tween-20 and 1% non-fat dry milk) and were added to the IgG or IgM-coated and blocked plates in 100 µl total volume. Plasma samples were heat inactivated prior to handling by incubating at 56°C for 30 min. Plasma samples were then diluted in dilution buffer starting at a 1:50 dilution, with an additional 7 two-fold serial dilutions. The diluted plasma samples, 27 from convalescent patients exposed to SARS-CoV-2 and 1 from a non-infected human control, were added to the plates in a total volume of 200 µl. After a two-hour incubation at RT, the plates were washed once with 150 µl of PBST by removing the samples and adding PBST by pipetting and subsequently washed 6 times using a gentle stream of deionized water from a faucet. Next, 100 µl anti-human IgG or IgM - horseradish peroxidase (HRP) conjugates (BioLegend), diluted 1:2500 and 1:5000 in dilution buffer, respectively, was added and the plates were incubated for 1 hour at RT. After four subsequent washes with deionized water 100 µl TMB (Thermo, cat. no. PI34024) was added and the plates were incubated in the dark at RT. The oxidation of TMB was stopped by adding 100 µl 0.18 M H_2SO_4 when the wells containing the most diluted IgG/IgM standard started to color. The absorbance was measured at 450 nm using a Synergy H4 Hybrid Plate Reader (BioTek). The average background signal of wells incubated without plasma was subtracted from the absorbance values for each sample. All plasma samples were measured in duplicate and the average absorbance reading was used to calculate the area under the curve using GraphPad 9.

Statistics

Statistical analyses were performed in GraphPad 9. Differences between two groups were evaluated using a Mann-Whitney U test. Differences in the expression of intracellular and cell

surface markers were tested using a Kruskal-Wallis test, followed by comparisons between selected pairs of groups using Dunn's post-hoc test, corrected for multiple comparisons. Non-parametric tests were used because the limited sample size did not allow for reliable evaluation of normal distribution and homoscedasticity.

Study approval

Samples and associated clinical data used in this study were received de-identified from the University of Texas Health San Antonio COVID-19 Repository. This repository was reviewed and approved by the University of Texas Health Science Center at San Antonio Institutional Review Board. All study participants provided written informed consent prior to specimen collection for the repository to include collection of associated clinical information and use of left-over clinical specimens for research. The COVID-19 Repository utilizes an honest broker system to maintain participant confidentiality and release of de-identified data or specimens to recipient investigators.

AUTHOR CONTRIBUTIONS

EMB secured funding for the study. RAR and EMB conceived the research question and designed the study. RAR isolated plasma and PBMCs, and acquired and analyzed flow cytometry data. KC performed and analyzed ELISAs. RAR, SB, and SJG produced S protein and RBD, which were purified by AMC. GC, RET, and TFP provided clinical samples and data. RG provided critical feedback on the manuscript. RAR, SB, and EMB wrote the manuscript with input from all other co-authors.

ACKNOWLEDGEMENTS

This work was supported by a COVID-19 pilot award from the UT Health Long School of Medicine (10009547 to E.M.B.). R.A.R. was supported by Translational Science Training award TL1 TR002647. Data were generated in the Flow Cytometry Shared Resource Facility, which is supported by UT Health, NIH-NCI P30 CA054174-20 (CTRC at UT Health) and UL1 TR001120 (CTSA grant). The following reagent was produced under HHSN272201400008C and obtained through BEI Resources, NIAID, NIH: Vector pCAGGS Containing the SARS-Related Coronavirus 2, Wuhan-Hu-1 spike glycoprotein receptor binding domain (RBD), NR-52309. SARS-CoV-2 spike HexaPro was a gift from Dr. Jason McLellan (Addgene plasmid #154754). The plasmid encoding BirA was a kind gift from Dr. Gavin Wright (Addgene plasmid # 32408).

REFERENCES

1. WHO Coronavirus Dashboard. Accessed September 17, 2021.
2. Goel RR, Apostolidis SA, Painter MM, Mathew D, Pattekar A, Kuthuru O, et al. Distinct antibody and memory B cell responses in SARS-CoV-2 naive and recovered individuals following mRNA vaccination. *Sci Immunol.* 2021;6(58).
3. Greaney AJ, Loes AN, Gentles LE, Crawford KHD, Starr TN, Malone KD, et al. Antibodies elicited by mRNA-1273 vaccination bind more broadly to the receptor binding domain than do those from SARS-CoV-2 infection. *Sci Transl Med.* 2021;13(600).
4. Dan JM, Mateus J, Kato Y, Hastie KM, Yu ED, Faliti CE, et al. Immunological memory to SARS-CoV-2 assessed for up to 8 months after infection. *Science.* 2021;371(6529).
5. Turner JS, Kim W, Kalaidina E, Goss CW, Rauseo AM, Schmitz AJ, et al. SARS-CoV-2 infection induces long-lived bone marrow plasma cells in humans. *Nature.* 2021;595(7867):421-5.
6. Hartley GE, Edwards ESJ, Aui PM, Varese N, Stojanovic S, McMahon J, et al. Rapid generation of durable B cell memory to SARS-CoV-2 spike and nucleocapsid proteins in COVID-19 and convalescence. *Sci Immunol.* 2020;5(54).
7. Wang Z, Muecksch F, Schaefer-Babajew D, Finkin S, Viant C, Gaebler C, et al. Naturally enhanced neutralizing breadth against SARS-CoV-2 one year after infection. *Nature.* 2021;595(7867):426-31.
8. Sokal A, Chappert P, Barba-Spaeth G, Roeser A, Fourati S, Azzaoui I, et al. Maturation and persistence of the anti-SARS-CoV-2 memory B cell response. *Cell.* 2021;184(5):1201-13 e14.
9. Lumley SF, O'Donnell D, Stoesser NE, Matthews PC, Howarth A, Hatch SB, et al. Antibody Status and Incidence of SARS-CoV-2 Infection in Health Care Workers. *N Engl J Med.* 2021;384(6):533-40.
10. Abu-Raddad LJ, Chemaitelly H, Coyle P, Malek JA, Ahmed AA, Mohamoud YA, et al. SARS-CoV-2 antibody-positivity protects against reinfection for at least seven months with 95% efficacy. *EClinicalMedicine.* 2021;35:100861.
11. Hansen CH, Michlmayr D, Gubbels SM, Molbak K, and Ethelberg S. Assessment of protection against reinfection with SARS-CoV-2 among 4 million PCR-tested individuals in Denmark in 2020: a population-level observational study. *Lancet.* 2021;397(10280):1204-12.
12. Grifoni A, Weiskopf D, Ramirez SI, Mateus J, Dan JM, Moderbacher CR, et al. Targets of T Cell Responses to SARS-CoV-2 Coronavirus in Humans with COVID-19 Disease and Unexposed Individuals. *Cell.* 2020;181(7):1489-501 e15.
13. Rodda LB, Netland J, Shehata L, Pruner KB, Morawski PA, Thouvenel CD, et al. Functional SARS-CoV-2-Specific Immune Memory Persists after Mild COVID-19. *Cell.* 2021;184(1):169-83 e17.
14. Roltgen K, and Boyd SD. Antibody and B cell responses to SARS-CoV-2 infection and vaccination. *Cell Host Microbe.* 2021;29(7):1063-75.
15. Seow J, Graham C, Merrick B, Acors S, Pickering S, Steel KJA, et al. Longitudinal observation and decline of neutralizing antibody responses in the three months following SARS-CoV-2 infection in humans. *Nat Microbiol.* 2020;5(12):1598-607.

16. Legros V, Denolly S, Vogrig M, Boson B, Siret E, Rigaill J, et al. A longitudinal study of SARS-CoV-2-infected patients reveals a high correlation between neutralizing antibodies and COVID-19 severity. *Cell Mol Immunol.* 2021;18(2):318-27.

17. Cohen KW, Linderman SL, Moodie Z, Czartoski J, Lai L, Mantus G, et al. Longitudinal analysis shows durable and broad immune memory after SARS-CoV-2 infection with persisting antibody responses and memory B and T cells. *Cell Rep Med.* 2021;2(7):100354.

18. Sandberg JT, Varnaite R, Christ W, Chen P, Muvva JR, Maleki KT, et al. SARS-CoV-2-specific humoral and cellular immunity persists through 9 months irrespective of COVID-19 severity at hospitalisation. *Clin Transl Immunology.* 2021;10(7):e1306.

19. Sakharkar M, Rappazzo CG, Wieland-Alter WF, Hsieh CL, Wrapp D, Esterman ES, et al. Prolonged evolution of the human B cell response to SARS-CoV-2 infection. *Sci Immunol.* 2021;6(56).

20. Muecksch F, Weisblum Y, Barnes CO, Schmidt F, Schaefer-Babajew D, Wang Z, et al. Affinity maturation of SARS-CoV-2 neutralizing antibodies confers potency, breadth, and resilience to viral escape mutations. *Immunity.* 2021;54(8):1853-68 e7.

21. Jenks SA, Cashman KS, Zumaquero E, Marigorta UM, Patel AV, Wang X, et al. Distinct Effector B Cells Induced by Unregulated Toll-like Receptor 7 Contribute to Pathogenic Responses in Systemic Lupus Erythematosus. *Immunity.* 2018;49(4):725-39 e6.

22. Woodruff MC, Ramonell RP, Nguyen DC, Cashman KS, Saini AS, Haddad NS, et al. Extrafollicular B cell responses correlate with neutralizing antibodies and morbidity in COVID-19. *Nat Immunol.* 2020;21(12):1506-16.

23. Stewart A, Ng JC, Wallis G, Tsioligka V, Fraternali F, and Dunn-Walters DK. Single-Cell Transcriptomic Analyses Define Distinct Peripheral B Cell Subsets and Discrete Development Pathways. *Front Immunol.* 2021;12:602539.

24. Kaneko N, Kuo HH, Boucau J, Farmer JR, Allard-Chamard H, Mahajan VS, et al. Loss of Bcl-6-Expressing T Follicular Helper Cells and Germinal Centers in COVID-19. *Cell.* 2020;183(1):143-57 e13.

25. Andrews SF, Chambers MJ, Schramm CA, Plyler J, Raab JE, Kanekiyo M, et al. Activation Dynamics and Immunoglobulin Evolution of Pre-existing and Newly Generated Human Memory B cell Responses to Influenza Hemagglutinin. *Immunity.* 2019;51(2):398-410 e5.

26. Lau D, Lan LY, Andrews SF, Henry C, Rojas KT, Neu KE, et al. Low CD21 expression defines a population of recent germinal center graduates primed for plasma cell differentiation. *Sci Immunol.* 2017;2(7).

27. Kim CC, Baccarella AM, Bayat A, Pepper M, and Fontana MF. FCRL5(+) Memory B Cells Exhibit Robust Recall Responses. *Cell Rep.* 2019;27(5):1446-60 e4.

28. Nellore A, Zumaquero E, Scharer CD, King RG, Tipton CM, Fucile CF, et al. Influenza-specific effector memory B cells predict long-lived antibody responses to vaccination in humans. *bioRxiv.*

29. Ogega CO, Skinner NE, Blair PW, Park HS, Littlefield K, Ganesan A, et al. Durable SARS-CoV-2 B cell immunity after mild or severe disease. *J Clin Invest.* 2021;131(7).

30. Beigel JH, Tomashek KM, Dodd LE, Mehta AK, Zingman BS, Kalil AC, et al. Remdesivir for the Treatment of Covid-19 - Final Report. *N Engl J Med.* 2020;383(19):1813-26.

686 31. Kalil AC, Patterson TF, Mehta AK, Tomashek KM, Wolfe CR, Ghazaryan V, et al.
687 Baricitinib plus Remdesivir for Hospitalized Adults with Covid-19. *N Engl J Med.*
688 2021;384(9):795-807.

689 32. Lucas C, Wong P, Klein J, Castro TBR, Silva J, Sundaram M, et al. Longitudinal analyses
690 reveal immunological misfiring in severe COVID-19. *Nature.* 2020;584(7821):463-9.

691 33. Oliviero B, Varchetta S, Mele D, Mantovani S, Cerino A, Perotti CG, et al. Expansion of
692 atypical memory B cells is a prominent feature of COVID-19. *Cell Mol Immunol.*
693 2020;17(10):1101-3.

694 34. Barnes CO, Jette CA, Abernathy ME, Dam KA, Esswein SR, Gristick HB, et al. SARS-
695 CoV-2 neutralizing antibody structures inform therapeutic strategies. *Nature.*
696 2020;588(7839):682-7.

697 35. Voss WN, Hou YJ, Johnson NV, Delidakis G, Kim JE, Javanmardi K, et al. Prevalent,
698 protective, and convergent IgG recognition of SARS-CoV-2 non-RBD spike epitopes.
699 *Science.* 2021;372(6546):1108-12.

700 36. Jaimes JA, Andre NM, Chappie JS, Millet JK, and Whittaker GR. Phylogenetic Analysis
701 and Structural Modeling of SARS-CoV-2 Spike Protein Reveals an Evolutionary Distinct
702 and Proteolytically Sensitive Activation Loop. *J Mol Biol.* 2020;432(10):3309-25.

703 37. Nguyen-Contant P, Embong AK, Kanagaiah P, Chaves FA, Yang H, Branche AR, et al. S
704 Protein-Reactive IgG and Memory B Cell Production after Human SARS-CoV-2 Infection
705 Includes Broad Reactivity to the S2 Subunit. *mBio.* 2020;11(5).

706 38. Ng KW, Faulkner N, Cornish GH, Rosa A, Harvey R, Hussain S, et al. Preexisting and de
707 novo humoral immunity to SARS-CoV-2 in humans. *Science.* 2020;370(6522):1339-43.

708 39. Wang C, van Haperen R, Gutierrez-Alvarez J, Li W, Okba NMA, Albulescu I, et al. A
709 conserved immunogenic and vulnerable site on the coronavirus spike protein delineated
710 by cross-reactive monoclonal antibodies. *Nat Commun.* 2021;12(1):1715.

711 40. Song G, He WT, Callaghan S, Anzanello F, Huang D, Ricketts J, et al. Cross-reactive
712 serum and memory B-cell responses to spike protein in SARS-CoV-2 and endemic
713 coronavirus infection. *Nat Commun.* 2021;12(1):2938.

714 41. Knox JJ, Buggert M, Kardava L, Seaton KE, Eller MA, Canaday DH, et al. T-bet+ B cells
715 are induced by human viral infections and dominate the HIV gp140 response. *JCI Insight.*
716 2017;2(8).

717 42. Newell KL, Clemmer DC, Cox JB, Kayode YI, Zoccoli-Rodriguez V, Taylor HE, et al.
718 Switched and unswitched memory B cells detected during SARS-CoV-2 convalescence
719 correlate with limited symptom duration. *PLoS One.* 2021;16(1):e0244855.

720 43. Hoehn KB, Ramanathan P, Unterman A, Sumida TS, Asashima H, Hafler DA, et al.
721 Cutting Edge: Distinct B Cell Repertoires Characterize Patients with Mild and Severe
722 COVID-19. *J Immunol.* 2021.

723 44. Lucas C, Klein J, Sundaram ME, Liu F, Wong P, Silva J, et al. Delayed production of
724 neutralizing antibodies correlates with fatal COVID-19. *Nat Med.* 2021;27(7):1178-86.

725 45. Ambegaonkar AA, Nagata S, Pierce SK, and Sohn H. The Differentiation in vitro of Human
726 Tonsil B Cells With the Phenotypic and Functional Characteristics of T-bet+ Atypical
727 Memory B Cells in Malaria. *Front Immunol.* 2019;10:852.

728 46. Zumaquero E, Stone SL, Scharer CD, Jenks SA, Nellore A, Mousseau B, et al. IFNgamma
729 induces epigenetic programming of human T-bet(hi) B cells and promotes TLR7/8 and IL-
730 21 induced differentiation. *Elife.* 2019;8.

731 47. Mohseni Afshar Z, Babazadeh A, Hasanpour A, Barary M, Sayad B, Janbakhsh A, et al.
732 Dermatological manifestations associated with COVID-19: A comprehensive review of the
733 current knowledge. *J Med Virol.* 2021;93(10):5756-67.

734 48. Blanco-Melo D, Nilsson-Payant BE, Liu WC, Uhl S, Hoagland D, Moller R, et al.
735 Imbalanced Host Response to SARS-CoV-2 Drives Development of COVID-19. *Cell.*
736 2020;181(5):1036-45 e9.

737 49. Johnson JL, Rosenthal RL, Knox JJ, Myles A, Naradikian MS, Madej J, et al. The
738 Transcription Factor T-bet Resolves Memory B Cell Subsets with Distinct Tissue
739 Distributions and Antibody Specificities in Mice and Humans. *Immunity.* 2020;52(5):842-55
740 e6.

741 50. Hsieh CL, Goldsmith JA, Schaub JM, DiVenere AM, Kuo HC, Javanmardi K, et al.
742 Structure-based design of prefusion-stabilized SARS-CoV-2 spikes. *Science.*
743 2020;369(6510):1501-5.

744

FIGURES

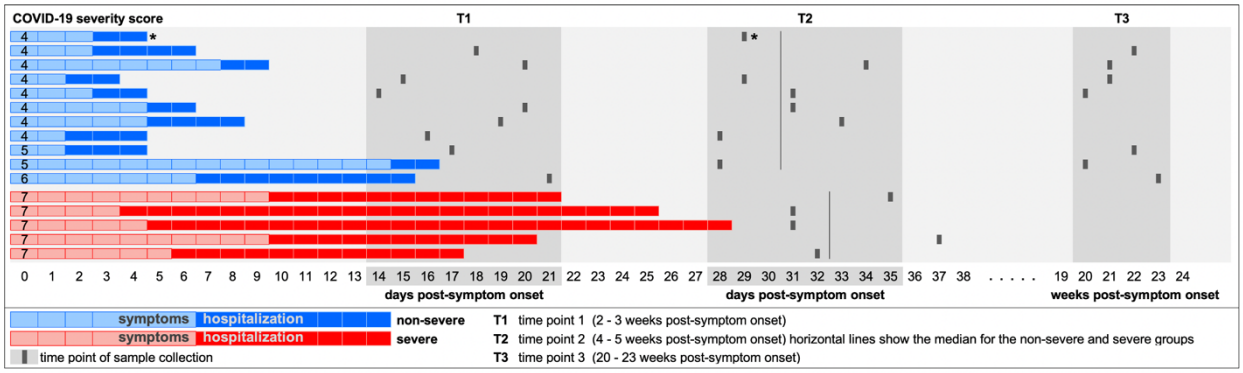

Figure 1: Timing of sample collection. Hospitalized COVID-19 patients were recruited for the study and sampled after hospital discharge. Samples from T2 were used for the comparison of B cell responses between individuals who recovered from non-severe and severe COVID-19 (**Figures 2 – 4**). All samples at T2 were collected 4 – 5 weeks post-symptom onset (PSO), with the exception of one severe donor who was sampled just after 5 weeks PSO (37 days). Longitudinal analysis of samples collected at T1 – T3 could only be performed for individuals who experienced non-severe disease, because the majority of severe patients were still hospitalized at T1 and we were unsuccessful in recruiting recovered severe patients for a follow-up blood draw at T3. The donor marked with * was included in the analysis of B cell subsets (**Figure 2**) and the percentage of spike-specific B cells (**Figure 3C**), but could not be included in all subsequent analyses because only a small number of spike-specific B cells (n = 6) was detected in this sample.

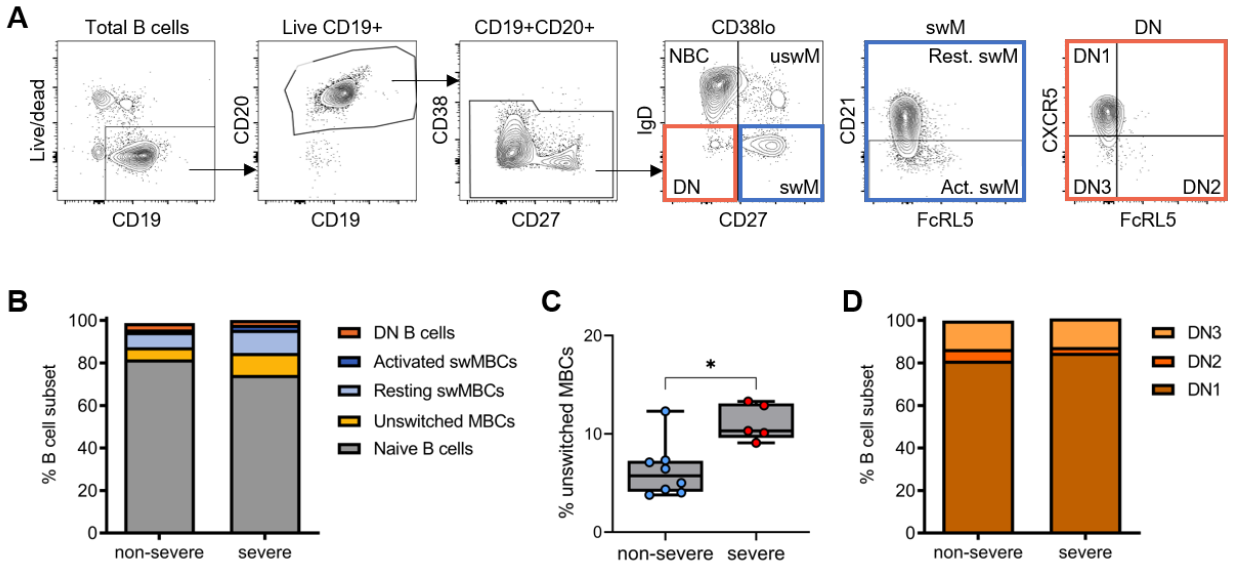

Figure 2: Distribution of major B cell subsets in recovered COVID-19 patients. A) Gating strategy to obtain non-antibody-secreting B cells (CD38lo) that are further divided into naïve, unswitched memory (uswM), switched memory (swM), and double negative (DN). SwM B cells were divided into activated and resting populations based on the expression of CD21. DN cells were divided into DN1 – 3 based on the expression of FcRL5 and CXCR5. **B)** Median percentage of each B cell subset in samples from individuals who recovered from non-severe COVID-19 and severe COVID-19. **C)** Percentage of unswitched memory B cells, which was increased in individuals who recovered from severe disease as compared to those who had non-severe COVID-19. **D)** Median proportions of the three different DN populations 1 month after non-severe or severe disease. In panel B – D, results are shown for individuals who recovered from non-severe COVID-19 (n = 8) and severe COVID-19 (n = 5). See **Figure S1** for graphs with individual data points for the data shown in panels B and D. * $P < 0.05$

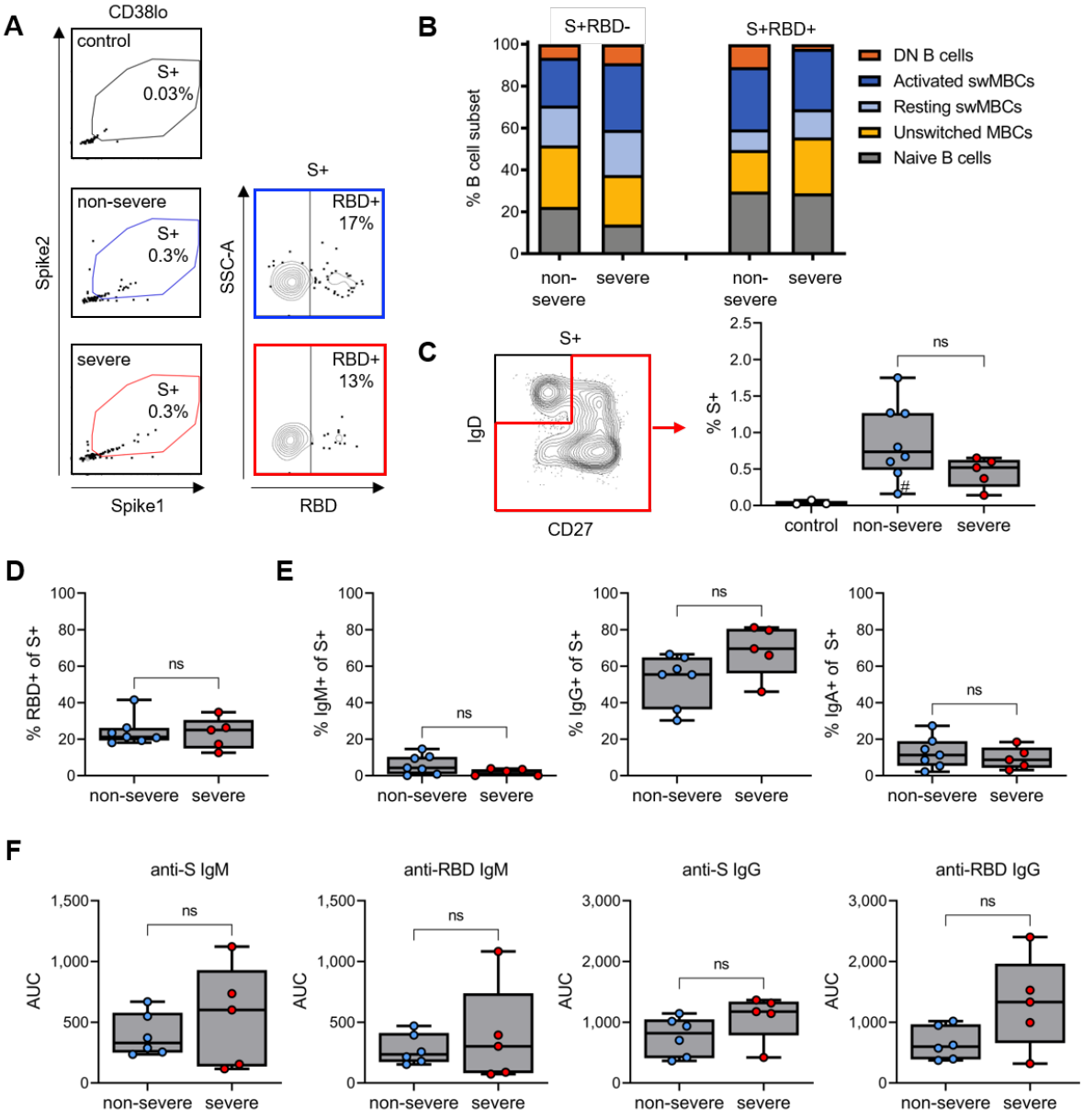

Figure 3: Detection of spike-specific and RBD-specific B cells and plasma antibody responses. A) Flow cytometry gating of spike-specific (S+) and RBD-specific (RBD+) B cells. **B)** Phenotype of non-RBD-specific (S+RBD-) and RBD-specific (S+RBD+) B cells, showing the median percentage among each group. Graphs with individual data points for each B cell subset are presented in **Figure S2**. **C)** Percentage of antigen-experienced spike-specific B cells in individuals who have never been exposed to SARS-CoV-2 (control) or who recovered from non-severe or severe disease. **D)** Percentage of spike-specific B cells that recognized RBD. **E)** Percentage of class-switched spike-specific B cells that express IgM (left), IgG (middle), or IgA (right). **F)** Plasma IgM (left) and IgG (right) titers against spike and RBD. Note that the range of the Y axes are different between IgM and IgG. In panel C, results are shown for individuals who recovered from non-severe COVID-19 (n = 8) and severe COVID-19 (n = 5). Only seven individuals with non-severe COVID-19 were included in panels B, D, and E, due to the low number of spike-specific B cells detected in the individual marked with # in panel C.

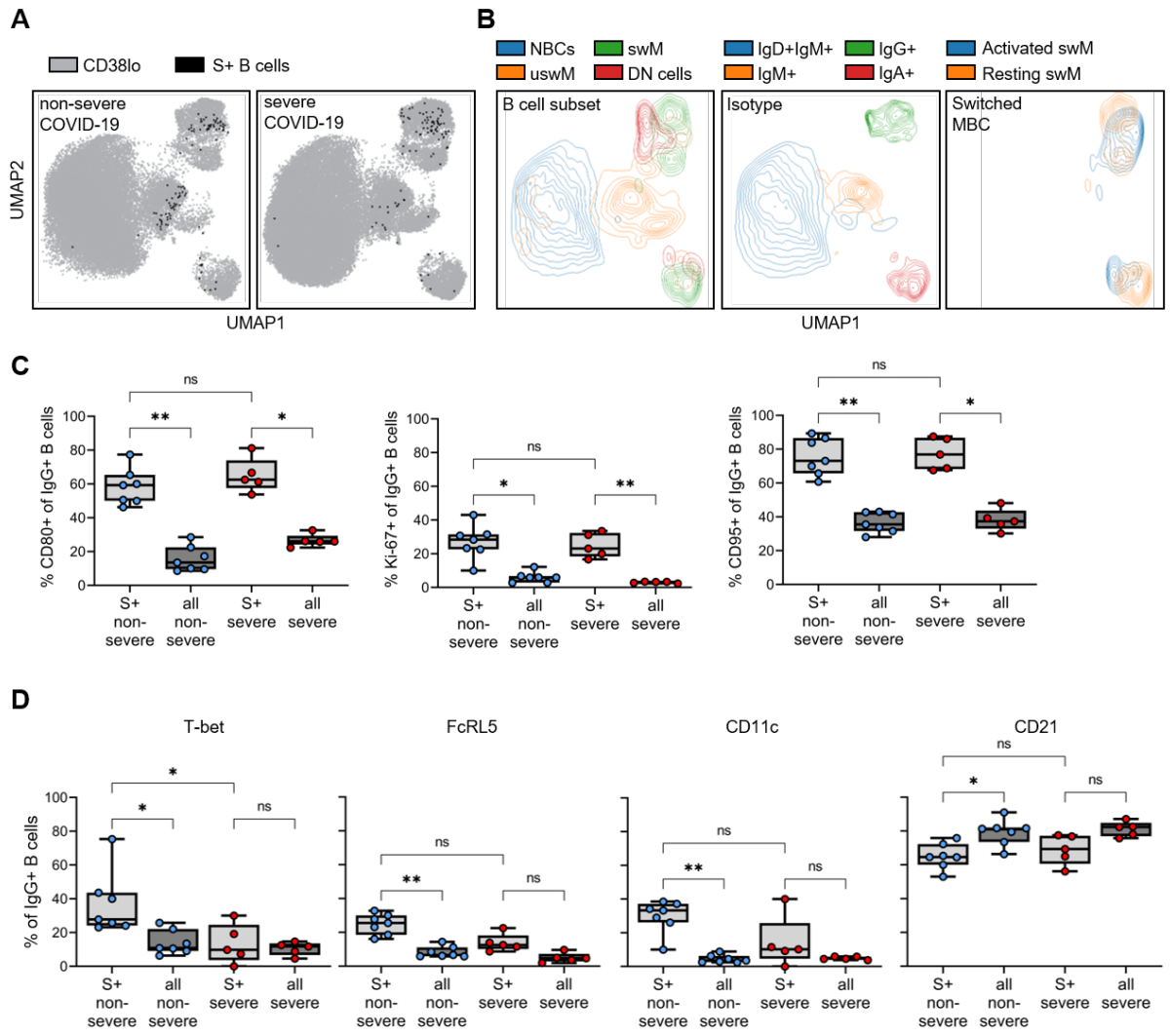

788

789 **Figure 4: Differences in the percentage spike-specific T-bet$^+$ B cells between patients**
790 **recovered from non-severe and severe COVID-19. A)** Composite UMAP showing the overlay
791 of spike-specific B cells from individuals who recovered from non-severe (left) or severe (right)
792 disease onto all B cells from that group. **B)** Overlay of major B cell subsets and isotypes onto
793 the composite UMAP. **C)** Expression of CD80, Ki-67, and CD95 by spike-specific (S+) IgG$^+$ B
794 cells and all IgG$^+$ B cells in individuals who experienced non-severe or severe COVID-19. **D)**
795 Expression of T-bet, FcRL5, CD11c, and CD21 by spike-specific IgG$^+$ B cells and all IgG$^+$ B
796 cells in individuals who experienced non-severe or severe COVID-19. Results are shown for
797 seven individuals who recovered from non-severe COVID-19 and five patients who recovered
798 from severe COVID-19. * P < 0.05; ** P < 0.01

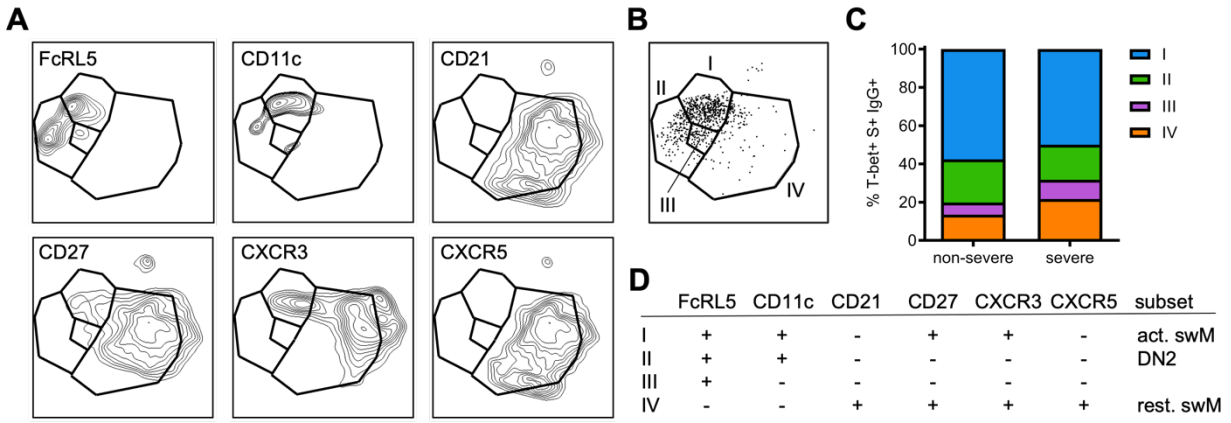

799

800 **Figure 5: The phenotype of T-bet$^+$ IgG$^+$ spike-specific B cells. A)** UMAPS showing the
801 expression of individual markers in T-bet$^+$ IgG$^+$ spike-specific B cells. **B)** Gating of four
802 populations of T-bet$^+$ IgG$^+$ B cells based on unique expression profiles of the markers shown in
803 panel A. **C)** Distribution of the four T-bet$^+$ IgG$^+$ B cell population among individuals who
804 recovered from non-severe (n = 7) and severe (n = 5) COVID-19. **D)** Summary of the phenotype
805 of the four T-bet$^+$ IgG$^+$ B cell populations identified here and their classification into one of the
806 major B cell subsets: activated switched memory (act. swM), DN2, or resting switched memory
807 (rest. swM) B cells.

808

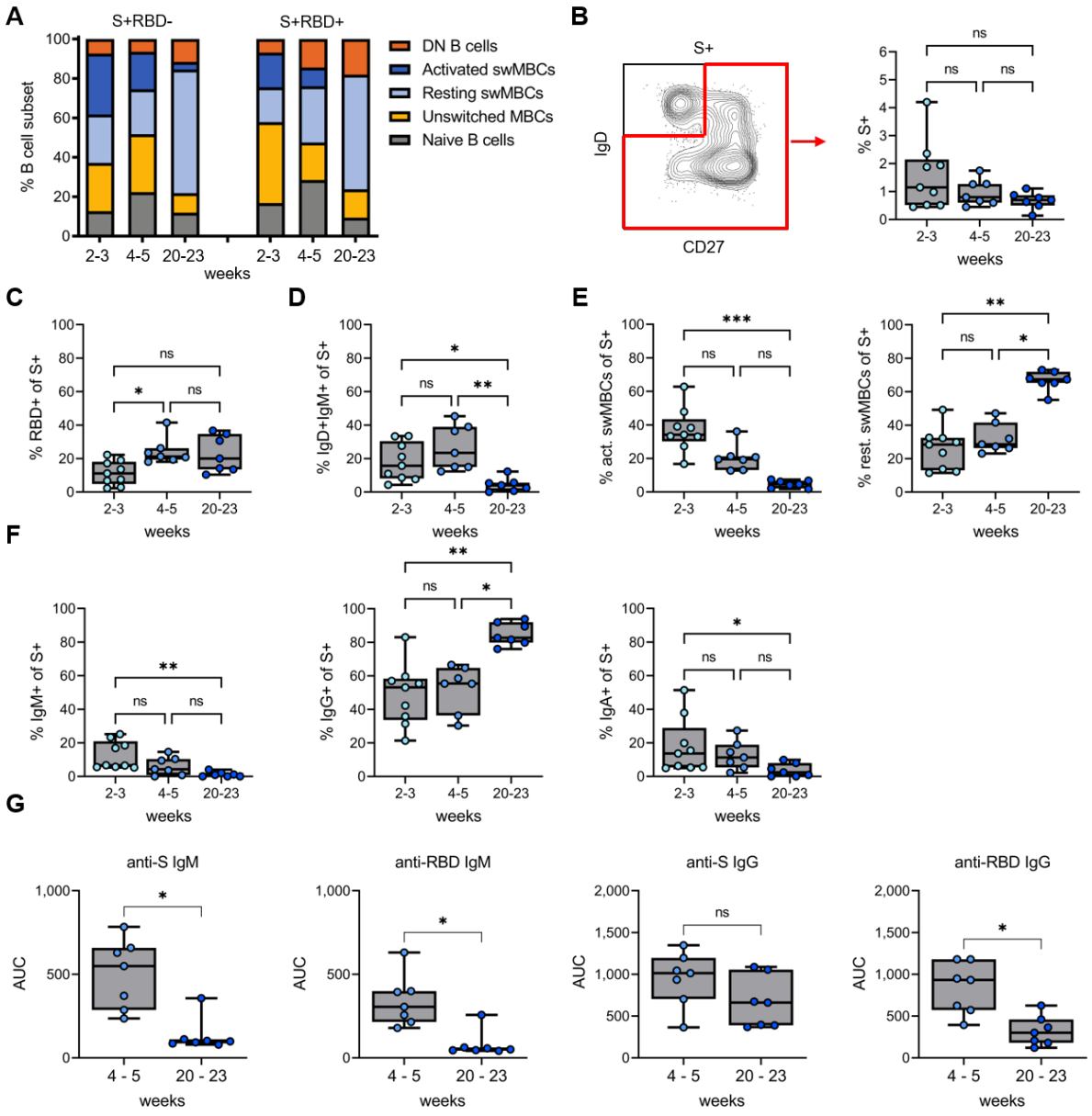

Figure 6: Change from activated to resting memory phenotype of IgG⁺ spike-specific B cells at five months post-symptom onset. A) Phenotype distribution of non-RBD-specific (S+RBD-) and RBD-specific (S+RBD+) B cells, showing the median percentage among each group. Graphs with individual data points for each B cell subset are presented in **Figure S6**. **B)** Percentage of antigen-experienced spike-specific B cells at 2 – 3, 4 – 5, and 20 – 23 weeks post-symptom onset. **C)** Percentage of S+RBD+ B cells among antigen-experienced spike-specific B cells. **D)** Percentage of unswitched memory B cells among antigen-experienced spike-specific B cells. **E)** Percentage of activated (left) and resting (right) switched memory B cells among antigen-experienced spike-specific B cells. **F)** Percentage of class-switched spike-specific B cells that express IgM (left), IgA (middle), or IgG (right). **G)** Plasma IgM (left) and IgG (right) titers against spike and RBD. In all panels, results are shown for samples collected 2 – 3 (n = 9), 4 – 5 (n = 7), and 20 – 23 (n = 7) weeks post-symptom onset. * P < 0.05; ** P < 0.01; *** P < 0.001

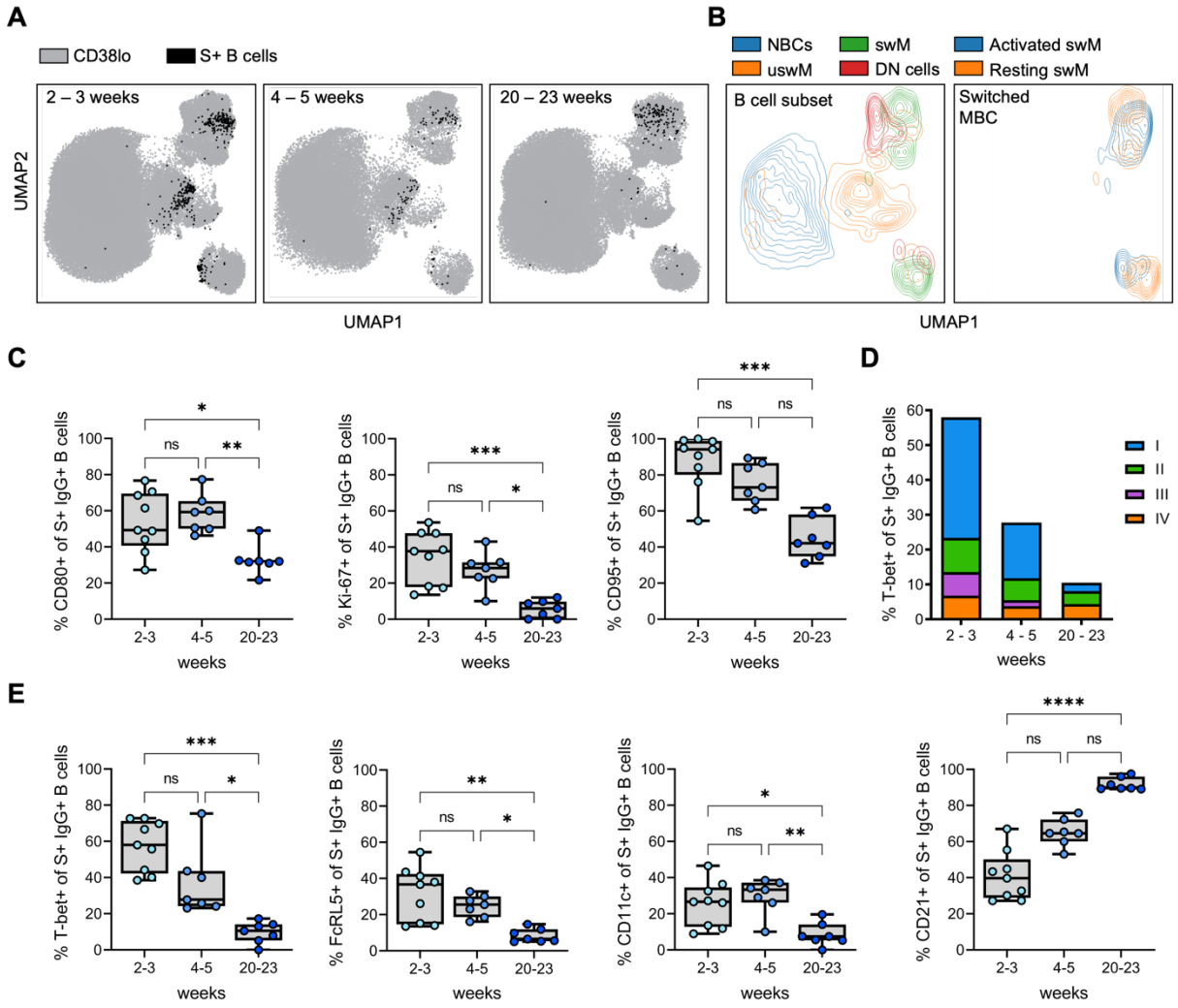

Figure 7: Longitudinal dynamics in the percentage of spike-specific B cells that express T-bet and various surface markers shortly after recovery and five months post-symptom onset. A) Composite UMAP showing the overlay of spike-specific B cells from individuals who recovered from non-severe COVID-19 at 2-3 (left), 4-5 (middle), and 20-23 (left) weeks post-symptom onset. **B)** Overlay of major B cell subsets and activated/resting switched memory B cells onto the composite UMAP. **C)** Expression of CD80, Ki-67, and CD95 by spike-specific (S+) IgG^+ B cells at the three time points. **D)** Distribution of the four $T\text{-}bet^+$ subsets (as defined in **Figure 5**) among spike-specific IgG^+ B cells at the three time points post-symptom onset. **E)** Expression of T-bet, FcRL5, CD11c, and CD21 by spike-specific IgG^+ B cells at the three time points post-symptom onset. In all graphs, results are shown for samples collected 2 – 3 (n = 9), 4 – 5 (n = 7), and 20 – 23 (n = 7) weeks post-symptom onset. * $P < 0.05$; ** $P < 0.01$; *** $P < 0.001$; **** $P < 0.0001$